Acta Polytechnica CTU Proceedings **37**:16–23, 2022
https://doi.org/10.14311/APP.2022.37.0016

Published by the Czech Technical University in Prague

DEGRADATION OF CR-COATED CLADDING UNDER THE SIMULATED LOSS-OF-COOLANT ACCIDENT PHENOMENA

Petr Červenka[a,b,*], Jakub Krejčí[b], Ladislav Cvrček[a], František Manoch[b], Adéla Chalupová[c], Patricie Halodová[d], Petra Gávelová[d]

[a] *Czech Technical University in Prague, Faculty of Mechanical Engineering, Department of Material Engineering, Karlovo náměstí 293/13, 120 00 Prague, Czech Republic*

[b] *UJP PRAHA a.s., Nad Kamínkou 1345, 156 00 Praha-Zbraslav, Czech Republic*

[c] *Czech Technical University in Prague, Faculty of Mechanical Engineering, Department of Energy Engineering, Technická 4, 166 07 Praha 6, Czech Republic*

[d] *Research Centre Řež s.r.o., Hlavní 130, Husinec – Řež, 250 68 Husinec, Czech Republic*

[*] corresponding author: p.cervenka@fs.cvut.cz

Abstract. The present study focuses on the evaluation of the mechanical properties degradation of Cr-coated Zr-alloy fuel cladding. The main objective of the work is to find a suitable methodology to evaluate the mechanical properties degradation of coated cladding by performing several separate effects experiments.

Apart from the many positive effects of protective coatings on the overall cladding properties, coatings' general disadvantage is their reduced ability to tolerate plastic strain. Therefore, coating cracks might occur in the first stage of the hypothetical Loss of Coolant Accident (LOCA). The study is unique because of the consideration of coating cracks. Prior to the high-temperature (HT) oxidation, samples were subjected to either a scratch test or burst test, resulting in the creation of coating defects. The subsequent evaluation of the obtained data consisted of wavelength dispersion spectroscopy (WDS) and optical microscopy analysis and hydrogen content measurements.

Keywords: ATF, LOCA, coating, oxidation, secondary hydriding, cladding embrittlement.

1. Introduction

Following the events at the Fukushima Daiichi (2011) power plant, substantial effort has been made studying the idea of Accident Tolerant Fuel (ATF), which would significantly enhance nuclear safety. In the past decade, a large variety of ATF concepts has been proposed and tested worldwide [1–9]. However, the most manageable and short-term approach to enhance the cladding performance is surface modification by specific technologies and various coatings.

In particular, metallic Cr has attracted many researchers due to its high melting point, superior corrosion resistance, good HT oxidation resistance, and similar thermal expansion coefficient of $6.2{\cdot}10^{-6}$ K^{-1} compared to Zr (i.e. $6{\cdot}10^{-6}$ K^{-1}) [10]. Cr-based coatings' good performance under both normal and accident conditions is based on the successful growth of a protective Cr_2O_3 scale. Cr coatings might significantly increase the fuel coping time by prolonging the oxidation time, which would lead to severe cladding embrittlement or even failure. It was confirmed as a promising ATF concept mitigating the main limitations of Zr cladding, such as fast degradation and an accelerated exothermic reaction with steam at high temperatures associated with hydrogen generation.

However, the HT oxidation experiments performed so far have focused mainly on the performance of the ideal coating without defects [11–14]. According to existing studies, the HT steam oxidation process of Cr-coated Zr-based alloys can be divided into three groups. Based on the duration and temperature of HT oxidation, the coating is protective, transition or no longer protective [15]. The protective coating features nearly parabolic oxidation kinetics with the growth of the outer protective Cr_2O_3 layer. The loss of protectiveness is characterized by the slow acceleration of oxidation kinetics, which is due to Zr diffusing outward along the Cr grain boundaries and in the opposite direction the Cr diffusing deeper into the β-Zr phase. Following the formation of the ZrO_2 layer along the Cr grain boundaries on the residual Cr scale, the inward diffusion of oxygen through the Zr network is induced. In the end, the coating loses its protective ability and the oxidation kinetics rapidly accelerates.

This work aims to evaluate the behavior of the coating in case of cracks present in the protective coating. Cracks in the coating may be formed, for instance, during fabrication, transportation, storing, normal operation (mostly grid-to-rod fretting, axial offset anomalies, etc.), or during a LOCA. In the event of LOCA in a pressurized water reactor, depressurization of the primary circuit may cause the fuel cladding to balloon as a result of internal pressure in

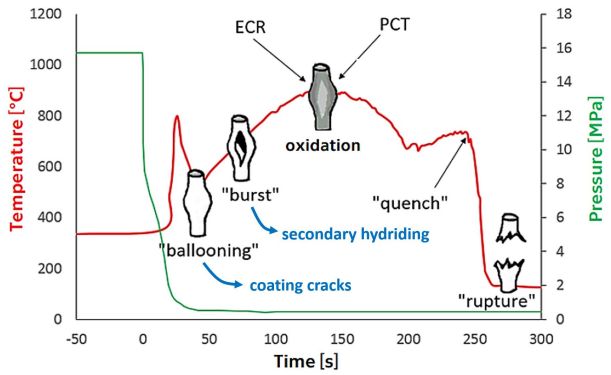

FIGURE 1. The schematic overview of LB-LOCA accident.

the fuel rods. The limited ability of the coating to tolerate plastic deformation leads to the formation of coating cracks. Details of the ballooning and burst phenomena were studied for various coatings [16].

Regarding accident conditions, massive hydrogen uptake should also be considered as a possible cause of cladding failure [17–20]. The secondary hydriding phenomenon might occur in HT transients (e.g., LOCA) due to the possible formation of burst openings after the ballooning phase (see Figure 1). The water steam flows through the burst area into the cladding. Since the flow is impeded by nuclear fuel pellets, there is steam starvation inside the cladding. As long as the steam flow remains sufficient, the inner oxidation is present, and the oxide layer forms a barrier against hydrogen ingress. Further from the burst opening, steam starvation might result in massive hydrogen uptake. Hydrogen concentrates in β-Zr phase (β-stabiliser) and can lead to cladding embrittlement due to the oxygen solubility increasing in β-Zr phase [21, 22].

It is important to note that the thin oxide layer formed inside the cladding during normal operation is not sufficient to prevent the cladding from hydrogen uptake [20]. At high temperatures, the oxygen diffusion inward to the Zr substrate can be assumed because of the high oxygen diffusion coefficients. In other words, the dissolution of the preexisting oxide layer is expected [23].

The preparation of the specimens and experimental procedures was carried out at UJP PRAHA in collaboration with CTU in Prague and Research Centre Řež. The main goal of this study is to verify additional mechanical properties degradation phenomena that might occur under accident conditions and can lead to sever cladding embrittlement.

2. Materials and methods

2.1. Preparation of specimens

All experiments were performed using standard Zr-based alloy as a reference material. The as-received fully recrystallized cladding rods had an outer diameter of 9.1 mm and a wall thickness of 0.57 mm.

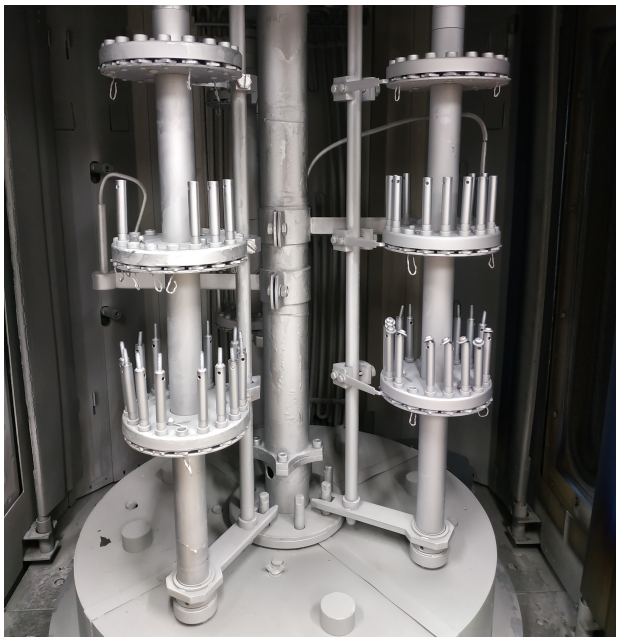

FIGURE 2. The chamber of the Hauzer Flexicoat 850 coating machine.

The non-irradiated segments used for the burst tests were 90 mm long, whereas the specimens used for the scratch tests were 45 mm long. All specimens were deburred and ultrasonically cleaned according to the standard procedure (3 × 10 minutes in acetone, ethanol and distilled water, respectively). Moreover, the surface of the specimens was cleaned in the first stage of the deposition process by ion etching in an argon plasma to remove all impurities and thin oxide layers.

2.2. Coating deposition

Pure chromium coatings were deposited on the outer surfaces of tubular samples. The deposition was carried out using an industrial Flexicoat 850 (Hauzer) system, see Figure 2. The facility may utilize different deposition techniques, such as sputtering, HIPIMS, PACVD, and others. However, the unbalanced magnetron sputtering was used to obtain a thin and fully dense microstructure free of defects. The deposition process was carried out using a target of 99,6 % Cr which was sputtered in the Ar atmosphere at 250 °C. The temperature of the process was lower than the temperature during normal operating conditions in the core, therefore thermal modification of specimens was avoided. The thicknesses of the as-deposited coatings were estimated using a Calotest (CSM Instruments), see Figure 3. The resulting coating thickness was approx. 20 µm depending on the particular batch.

2.3. Experimental methods

In studying the effect of scratches on cladding degradation, two different surface damage techniques were used. The first method consisted of creating artificial defects, that is, scratches through the protective scale,

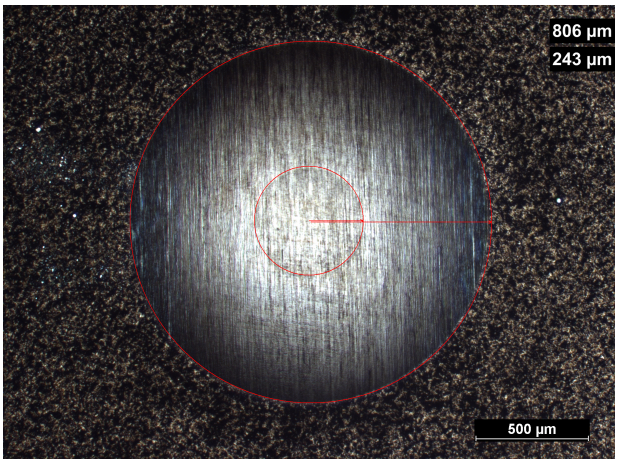

Figure 3. Calotest.

on a scratch test device. This test allowed the creation of individual defects, which set optimal conditions for the detailed study of diffusion processes through the damaged coating during subsequent HT oxidation. The second batch of specimens was damaged naturally by the ballooning process due to internal pressure.

Afterward, each specimen was subjected to HT oxidation in Ar + steam to simulate the LOCA scenario. The subsequent analyses focused on the diffusive process of Cr into the Zr substrate and the secondary hydriding phenomenon.

2.3.1. Scratch test

The first batch of Cr-coated specimens was artificially pre-damaged to simulate cracking of the coating layer during the HT transient. Using the Revetest Xpress device (CSM Instruments) with a standard Rockwell diamond indenter, several scratches through the coating layer were made. Scratches 40 mm in length were made at the speed of 20 mm·min^{-1} using the constant load of 50 N. The scratch test process is shown in Figure 4. The resulting U-shaped scratches were 200 µm wide.

2.3.2. Ballooning and burst test

The ballooning was performed in a burst test facility consisting of a resistance furnace, temperature controller, and Argon containing reservoir to pressurize the specimen. The specimens were sealed using endplugs and connected to the Argon-containing reservoir. Each specimen was equipped with a pair of K-thermocouples – one attached next to the specimen's surface and the second welded directly to the specimen.

Various methods may be chosen to perform the burst test. A RAMP test, the course of which is visualized in Figure 5, was selected. First, the specimen was preheated at 360 °C and pressurized to an inner pressure of 4 MPa. Then, the pressurized specimen was heated at a heating rate of 7 °C·s^{-1} until its failure (899 °C). A constant flow of Argon was induced to the retort throughout the experiment to prevent HT

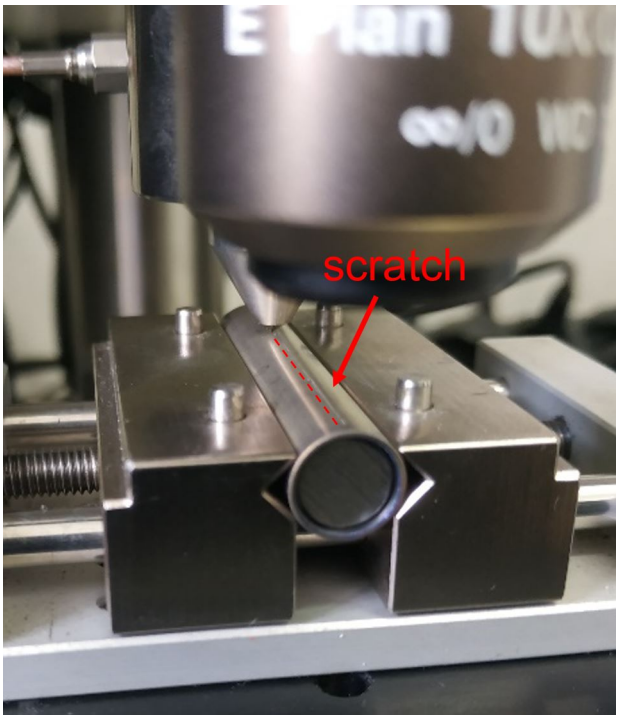

Figure 4. Scratch Test Revetest Xpress.

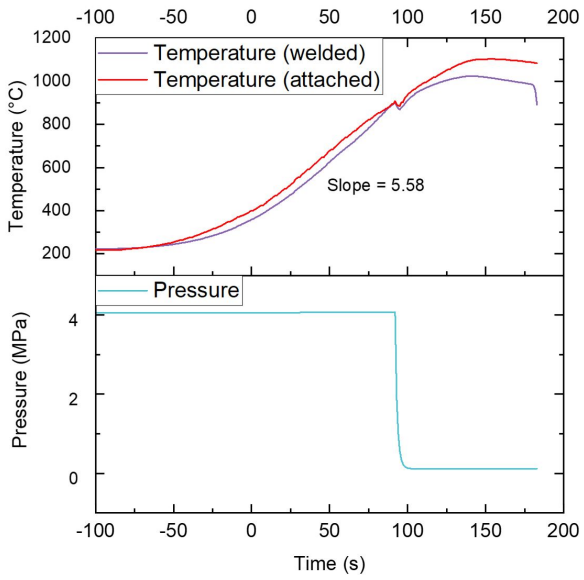

Figure 5. Time course of the burst test.

oxidation. After the test, the specimens were visually analyzed and photographed. Subsequently, the time to burst, the deformation, and the creep rate were evaluated.

2.3.3. High-temperature oxidation

The experiment of HT oxidation was performed in the electric resistant furnace in the Ar + steam mixture according to the scheme shown in Figure 6. The steam atmosphere is typical for DBAs such as LOCA. In addition to that, steam oxidation might be followed by secondary hydriding, a phenomenon that might occur in the cladding after burst due to inner oxidation and

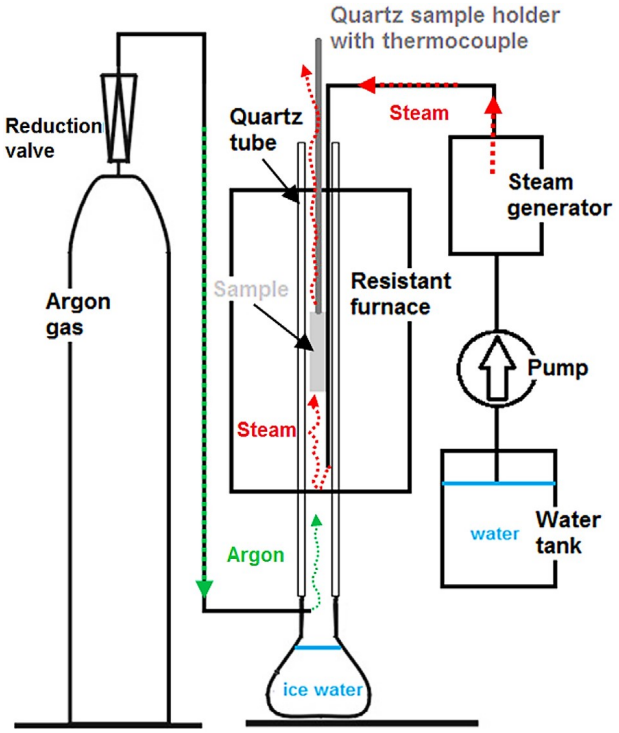

FIGURE 6. Schematic of the facility for the HT oxidation experiment.

steam starvation.

The experiment was conducted at the temperature of 1200 °C, which is considered the highest temperature of design basis accidents. The temperature was measured by the thermocouple placed inside the cladding tube in case there were no end caps on the specimen (i.e., specimens after scratch test, Figure 4). Specimens predamaged by the burst test were tested for oxidation and secondary hydriding, thus they were filled with ZrO_2 pellets and sealed with end plugs to impede the steam flow inside the cladding. The schematic overview is shown in Figure 7. The temperature in these experiments was measured by the thermocouple placed next to the outer cladding surface.

Experiments were performed following this procedure. First, the atmospheric gases were removed from the preheated furnace by a constant flow of Ar for 5 minutes. Then, the flow of Ar + steam stabilized the homogeneous conditions inside the quartz tube for 5 minutes. Finally, the specimen was inserted into the furnace within the predefined temperature zone (±3 °C). The duration of HT oxidation ranged from 90 seconds to 9 minutes. Each experiment was terminated by iced water quenching. The reason behind this is that quenching directly from the oxidation temperature to 0 °C is a less conservative approach, more demanding on the mechanical properties.

2.3.4. Material characterization

Before and after each experiment, the specimen was weighed with Mettler Toledo XS105 semi-micro balance with the readability of 0,01 mg. Furthermore, the longitudinal dimensions were measured using an electronic caliper with an accuracy of 0,02 mm. The diameter was measured with a micrometer with an accuracy of 0,002 mm. After evaluation in the whole state, the specimens were cut into smaller pieces (rings) to perform additional analyzes.

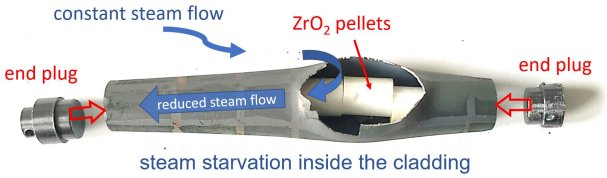

FIGURE 7. Schematic overview of the secondary hydriding after burst test experiment.

FIGURE 8. Ring segments cut for microscopy analysis.

Specimens with single cracks made on the scratch test device were observed using the scanning electron microscope (SEM) with a Field Emission Gun operated at an accelerating voltage of 15 kV. The test aimed to observe and evaluate diffusive processes through the damaged coating and the distribution of chemical composition in the affected area. The distribution profiles of Zr, Cr, O, N, and Fe were obtained from wavelength dispersion spectroscopy (WDS) analysis. The spectra were automatically processed by IncaWave software. The WDS chemical composition profiles were measured in two directions – perpendicular to the coating surface in the area not directly affected by the defect and parallel to the coating surface at the distance of 25 µm.

Regarding the HT oxidation after the burst experiments, the specimens were cut according to the following procedure. The first segment was cut in the middle of the burst, the second segment was located 10 mm from the burst opening and the third segment was located 20 mm from the burst opening, see Figure 8. Moreover, the hydrogen content was measured on a small part of each of these segments using the G8 Galileo (Bruker) analyzer. The Inert Gas Fusion (IGF) technique is based on fusing the tested macroscopic sample and thus is limited to obtaining only the peak hydrogen content, not its distribution.

3. Results

In this section, the results are shown and commented. First, WDS profiles of artificially predamaged (scratched) specimens are presented. Then the results of the HT oxidation after the burst test

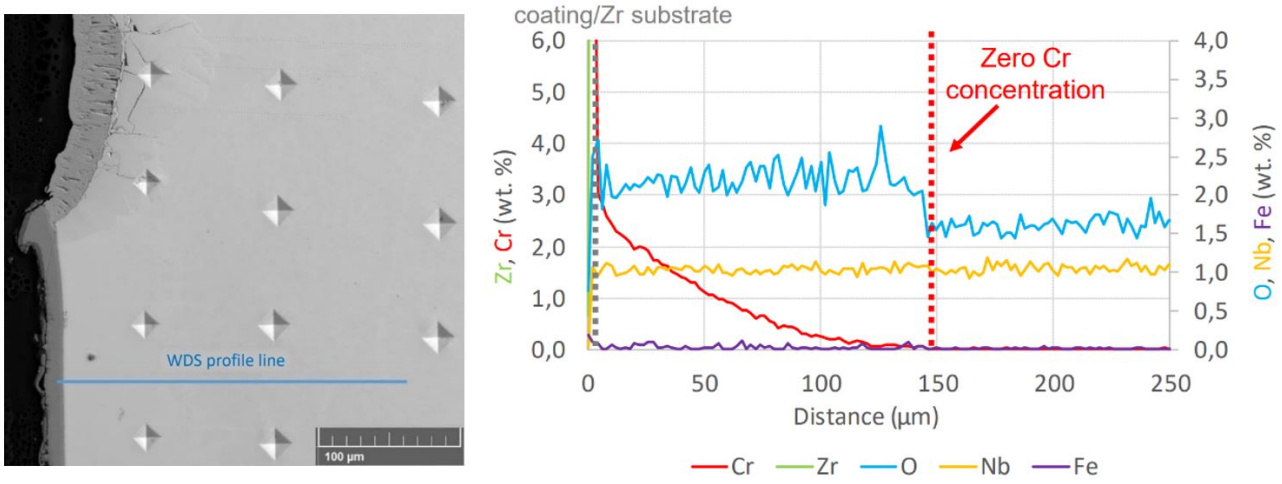

Figure 9. WDS composition profile perpendicular to the coating, 4,5 min HT oxidation.

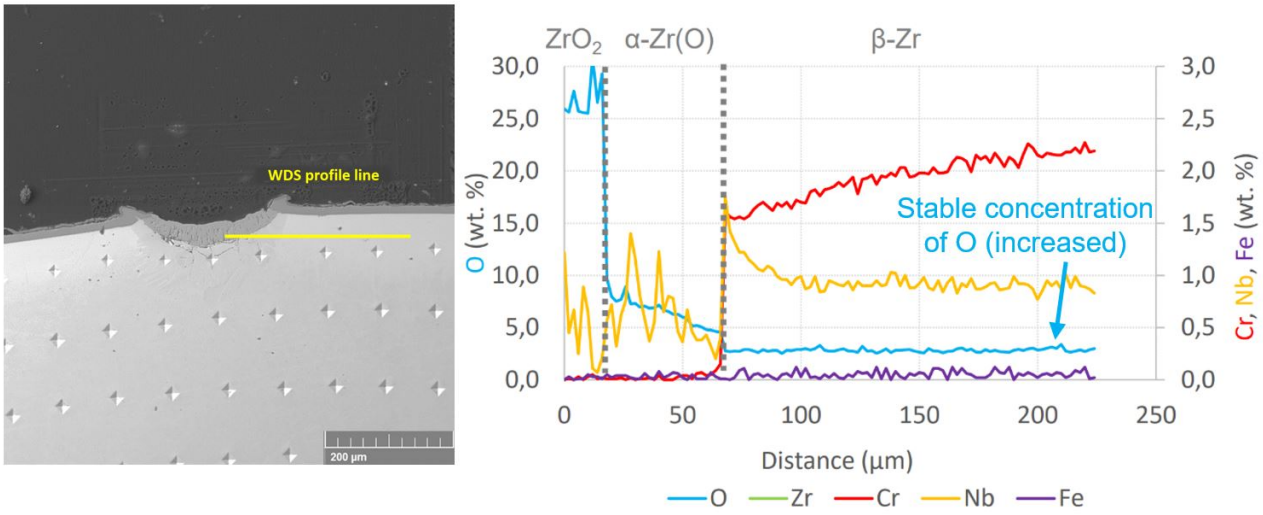

Figure 10. WDS profile measured parallel to the coating at a distance of 25 µm, 4,5 min HT oxidation.

are presented; first, the optical microscopy structure is discussed and then the measured hydrogen content is shown.

3.1. Chemical Analysis – HT oxidation after scratch test

The chemical composition measured perpendicular to the outer surface (blue line, Figure 9) clearly shows the diffusion of Cr from the coating inwards the Zr substrate. After a 4,5-minute exposition at 1200 °C, the Cr diffused approx. 150 µm in an inward direction. As long as there was some amount of Cr diffused, the measured content of oxygen remained stable yet increased, i.e. approx. at 2–2,5 %. Once the zero value of Cr is reached, the content of diffused oxygen drops significantly to 1,5–2 %.

The same, i.e., stable yet increased, oxygen content (∼2–2,5 %) was also measured in a parallel line to the outer surface (yellow line, Figure 10). There was no noticeable gradient of oxygen concentration along the entire length of the measured β-Zr section.

3.2. Metallography – secondary hydriding

The detailed microstructure of all 3 segments is shown in Figure 11. Cracking of the coating formed within the ballooning and burst test is apparent. The number of coating cracks depended on the size of the deformation. Therefore, the segment 1 with the highest deformation had the largest number of coating cracks. Furthermore, part of segment 1 near the burst opening consisted of a noticeably thinned cladding wall due to deformation in the ballooning phase. Finally, segment 3 located 20 mm from the burst opening featured substantially fewer uniformly distributed small cracks.

In the microstructure of segment 1, a massive growth of the α-Zr(O) can be seen. The Cr scale is massively cracked and there are no β-Zr sections directly under the coating. On the other hand, segments 2 and 3 contained significantly fewer coating cracks, which contributed to the formation of β-Zr segments in between. The growth of α-Zr(O) grains from defects was apparent in the inward direction. Due

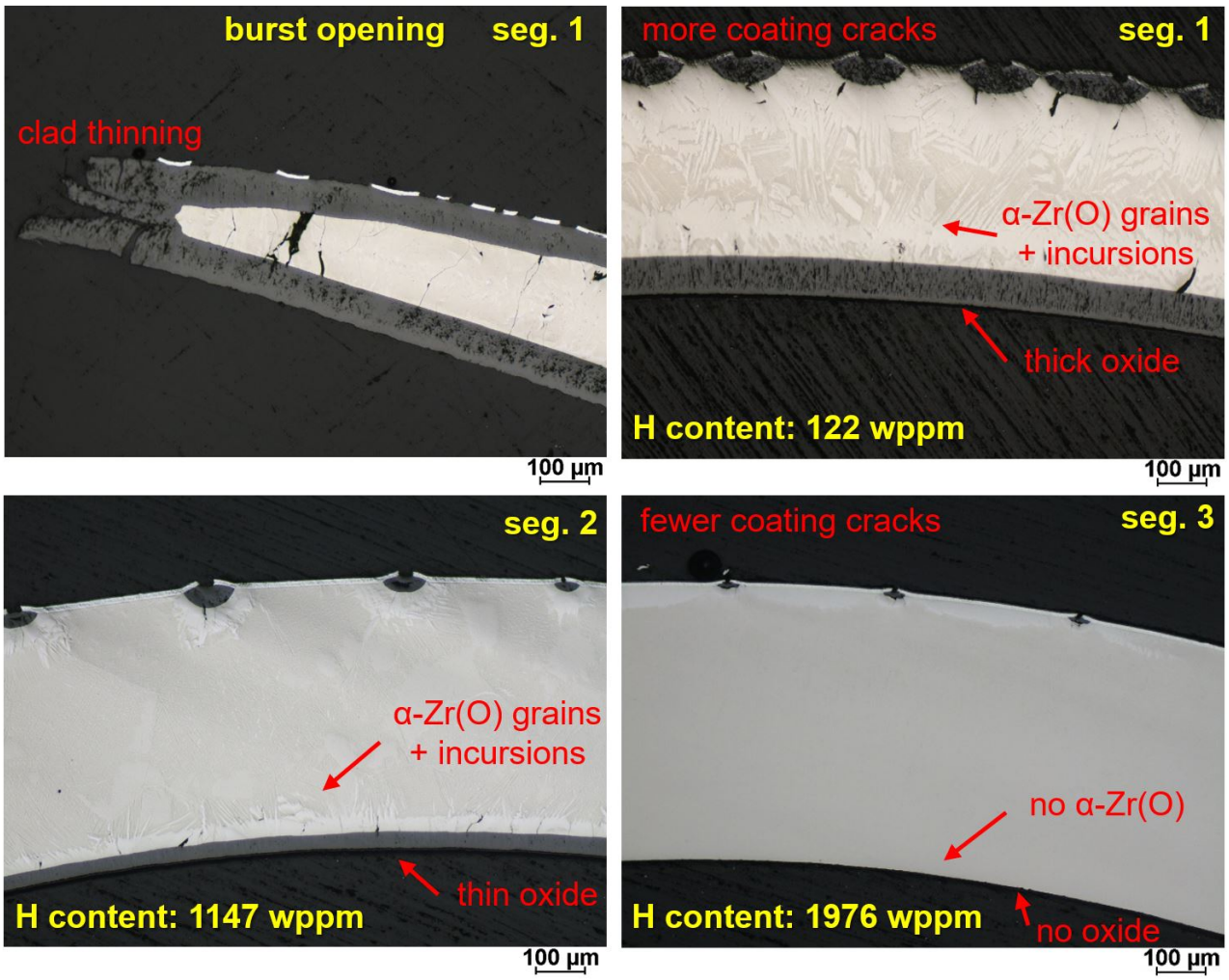

FIGURE 11. Results of secondary hydriding experiments.

to the Cr stabilizing the β-Zr phase, no growth of α-Zr(O) grains was observed in the tangential direction, in other words, there was no α-Zr(O) grains growth under the Cr scale. The Cr enriched β-Zr phase itself can be slightly seen, however, the true evidence of the Cr diffusion inwards the substrate remains the WDS analysis.

Regarding the internal oxidation, the decreasing thickness of the oxide layer further from the burst opening was evident. Furthermore, the growth of α-Zr(O) grains + α-Zr(O) grain incursions inwards was less evident further from the burst area, and additionally, in segment 3 was not observed at all.

3.3. Hydrogen content – secondary hydriding

Following the expected consequences of the secondary hydriding phenomenon, the hydrogen content grew with increasing distance from the burst opening (see Figure 11). While a very low hydrogen content (122 wppm) was measured at the area of the burst (i.e. segment 1), it considerably increased in segments 2 and 3. Particularly, the hydrogen content measured at a distance of 20 mm from the burst opening reached almost 2000 wppm.

4. Discussion

While the positive effect of undamaged Cr coating on oxidation performance has been widely presented and indeed remains undeniable, additional phenomena must be taken into account when evaluating coated cladding embrittlement.

It was observed that the Cr content led to increased oxygen solubility in the substrate (Figure 9). Since the oxygen content was at the same level throughout the measured β-Zr section (Figure 10), it can be concluded that loss of protectiveness of the coating and therefore diffusion of oxygen through the coating would not be the only mechanism of degradation of the coating. Apart from the inward growth of α-Zr(O) grains from the coating defect, which can be evaluated using optical microscopy methods and seem to be very local (as discussed, e.g. in Brachet's study [24]), the considerable amount of oxygen rapidly diffused into the Cr-enriched substrate. The reason behind this is Cr stabilizing the β-Zr phase. The diffusion coefficient of oxygen in β-Zr is much higher compared to α-Zr(O) phase [25, 26] resulting in the accelerated

oxygen dissolution in the Cr-stabilized β-Zr phase. Therefore, the impact of the coating defects cannot be excluded as the oxygen rapidly diffuses along the whole Cr scale.

On the basis of the results presented, it can be assumed that the impact of oxygen diffusion through the coated cladding upon accidents such as LOCA cannot be described only by looking at the protectiveness of the coating itself. The methodology must take into account the coating cracks that occur in the ballooning phase. They will lead to an accelerated diffusion of oxygen over the HT transient. The β-Zr phase will be affected. As a result, the load-bearing ability can be significantly reduced even under conditions (temperature, time) so far believed not to result in the loss of coating protectiveness.

The separate-effects-combining study confirmed the secondary hydriding phenomenon occurring in Cr-coated Zr-based cladding exposed to the ballooning and burst experiment first and then HT oxidized in Ar + steam. The hydrogen content measured in segment 2 and especially in segment 3 was high enough to increase the solubility of oxygen. Especially in the load-bearing prior β-Zr phase, such hydrogen uptake can result in cladding failure and must be taken into account.

5. Conclusion

To summarize the observations, using the Cr-coated standard Zr cladding alloy, separate effects experiments were performed. Specifically, ballooning and burst, HT Ar + steam oxidation, and secondary hydriding (HT oxidation after burst). The study was unique considering the cracking of the coating that occurred in the first stage of the hypothetical accident. The WDS analysis proved the Cr diffusion into the β-Zr substrate leading to accelerated diffusion of oxygen and its increased concentration even under the coated (thus so far believed to be protected) areas. Accelerated diffusion of oxygen, as well as its increased solubility, can affect mechanical properties. In particular, the ductility of the residual prior β-Zr phase, which is essential to maintain the integrity of the cladding, can be reduced. Therefore, it is necessary to consider the cracking of the coating when evaluating the degradation processes of the coated cladding.

The secondary hydriding phenomenon was observed when HT oxidation was performed using the specimens after ballooning and burst test. Massive H uptake (2000 wppm) occurred at a distance of 20 mm from the burst opening. The larger the deformation, the more cracks occurred in the Cr scale. Additionally, significant clad thinning was observed near the burst opening area. The hydrogen content measurement has been limited to macroscopic samples. Its detailed distribution across the cladding wall remains a matter of concern, since absorbed hydrogen can increase the oxygen solubility in β-Zr and have a huge impact on mechanical properties, i.e., on the cladding embrittlement.

While uncoated Zr-based claddings and their post-accident properties can be evaluated using standard methodology, such testing is not suitable for Cr-coated claddings due to more phenomena that must be taken into account. As the coating cannot withstand high plastic strain, various cracks in the Cr scale are likely to occur during heat-up. Moreover, in the case of a burst, local massive hydrogen uptake must be considered. It can be concluded that evaluating Cr-coated Zr cladding embrittlement requires complex testing that includes all of the LOCA phenomena, respectively.

Acknowledgements

The authors wish to thank the whole Zirconium Alloys Team at UJP PRAHA a.s. for sample preparation and post-experimental analyses. Special thanks to P. Halodová and P. Gávelová (Research Centre Řež s.r.o.) for performing the SEM analysis, and Ladislav Cvrček (CTU in Prague) for chromium coating deposition. The financial support of this research through ČEZ a.s. company is gratefully acknowledged. Also, this work was supported by the Institutional Support by Ministry of Industry and Trade, Technology Agency of the Czech Republic grant No. TK03020169.

References

[1] S. Zinkle, K. Terrani, J. Gehin, et al. Accident tolerant fuels for LWRs: A perspective. *Journal of Nuclear Materials* **448**(1):374–379, 2014. https://doi.org/10.1016/j.jnucmat.2013.12.005.

[2] K. Terrani. Accident tolerant fuel cladding development: Promise, status, and challenges. *Journal of Nuclear Materials* **501**:13–30, 2018. https://doi.org/10.1016/j.jnucmat.2017.12.043.

[3] L. Braase. Enhanced Accident Tolerant LWR Fuels National Metrics Workshop Report. Tech. rep., 2013. https://doi.org/10.2172/1073785.

[4] *Accident Tolerant Fuel Concepts for Light Water Reactors*. No. 1797 in TECDOC Series. International Atomic Eenergy Agency, Vienna, 2016.

[5] C. Tang, M. Stueber, H. Seifert, M. Steinbrück. Protective coatings on zirconium-based alloys as accident-tolerant fuel (ATF) claddings. *Corrosion Reviews* **35**(3), 2017. https://doi.org/10.1515/corrrev-2017-0010.

[6] M. Ševeček, J. Krejčí, A. Chalupová, et al. Round Robin Exercise of the Candidate ATF Cladding Materials Within the ACTOF Project. In *Top Fuel 2019, American Nuclear Society, Seattle, WA, September, 22-26*, pp. 283–290. Greyden Press, 2019. 32.02.11; LK 01.

[7] J. Krejčí, J. Kabátová, F. Manoch, et al. Development and testing of multicomponent fuel cladding with enhanced accidental performance. *Nuclear Engineering and Technology* **52**(3):597–609, 2020. https://doi.org/10.1016/j.net.2019.08.015.

[8] P. Červenka, J. Krejčí, L. Cvrček, et al. Experimental study of damaged Cr-coated fuel cladding in post-accident conditions. *Acta Polytechnica CTU*

Proceedings **28**:1–7, 2020. https://doi.org/10.14311/APP.2020.28.0001.

[9] J. Bischoff, C. Delafoy, C. Vauglin, et al. AREVA NP's enhanced accident-tolerant fuel developments: Focus on Cr-coated M5 cladding. *Nuclear Engineering and Technology* **50**(2):223–228, 2018. Special issue on the water reactor fuel performance meeting 2017 (WRFPM 2017), https://doi.org/10.1016/j.net.2017.12.004.

[10] H. Chen, X. Wang, R. Zhang. Application and Development Progress of Cr-Based Surface Coating in Nuclear Fuel Elements: II. Current Status and Shortcomings of Performance Studies. *Coatings* **10**:835, 2020. https://doi.org/10.3390/coatings10090835.

[11] B. Maier, H. Yeom, G. Johnson, et al. Development of cold spray chromium coatings for improved accident tolerant zirconium-alloy cladding. *Journal of Nuclear Materials* **519**:247–254, 2019. https://doi.org/10.1016/j.jnucmat.2019.03.039.

[12] A. Michau, F. Maury, F. Schuster, et al. High-temperature oxidation resistance of chromium-based coatings deposited by DLI-MOCVD for enhanced protection of the inner surface of long tubes. *Surface and Coatings Technology* **349**:1048–1057, 2018. https://doi.org/10.1016/j.surfcoat.2018.05.088.

[13] S. Kuprin, V. Belous, V. Voyevodin, et al. Vacuum-arc chromium-based coatings for protection of zirconium alloys from the high-temperature oxidation in air. *Journal of Nuclear Materials* **465**:400–406, 2015. https://doi.org/10.1016/j.jnucmat.2015.06.016.

[14] Z. Yang, Y. Niu, J. Xue, et al. Steam oxidation resistance of plasma sprayed chromium-containing coatings at 1200 °C. *Materials and Corrosion* **70**(1):37–47, 2019. https://doi.org/10.1002/maco.201810156.

[15] J.-C. Brachet, E. Rouesne, J. Ribis, et al. High temperature steam oxidation of chromium-coated zirconium-based alloys: Kinetics and process. *Corrosion Science* **167**:108537, 2020. https://doi.org/10.1016/j.corsci.2020.108537.

[16] A. Chalupová, J. Krejčí, L. Cvrček, et al. Coated cladding behavior during high-temperature transients. *Acta Polytechnica CTU Proceedings* **24**:9–14, 2019. https://doi.org/10.14311/APP.2019.24.0009.

[17] I. Turque, R. Chosson, M. Le Saux, et al. Mechanical behavior at high temperature of highly oxygen- or hydrogen-enriched α and (prior-) β phases of zirconium alloys. pp. 240–280. 2018. https://doi.org/10.1520/STP159720160063.

[18] Z. Hózer, I. Nagy, A. Vimi, et al. *High-Temperature Secondary Hydriding Experiments with E110 and E110G Claddings*, pp. 1093–1113. 2018. ISBN 978-0-8031-7641-6, https://doi.org/10.1520/STP159720160031.

[19] J. Stuckert, M. Große, C. Rössger, et al. QUENCH-LOCA program at KIT on secondary hydriding and results of the commissioning bundle test QUENCH-L0. *Nuclear Engineering and Design* **255**:185–201, 2013. https://doi.org/10.1016/j.nucengdes.2012.10.024.

[20] J.-C. Brachet, D. Hamon, M. Le Saux, et al. Study of secondary hydriding at high temperature in zirconium based nuclear fuel cladding tubes by coupling information from neutron radiography/tomography, electron probe micro analysis, micro elastic recoil detection analysis and laser induced breakdown spectroscopy microprobe. *Journal of Nuclear Materials* **488**:267–286, 2017. https://doi.org/10.1016/j.jnucmat.2017.03.009.

[21] S. Guilbert-Banti, P. Lacote, G. Taraud, et al. Influence of hydrogen on the oxygen solubility in Zircaloy-4. *Journal of Nuclear Materials* **469**:228–236, 2016. https://doi.org/10.1016/j.jnucmat.2015.11.019.

[22] L. Portier, T. Bredel, J. C. Brachet, et al. Influence of long service exposures on the thermal-mechanical behavior of Zy-4 and M5™ alloys in LOCA conditions. In *Zirconium in the Nuclear Industry: Fourteenth International Symposium*, pp. 896–920. ASTM International, 2005. https://doi.org/10.1520/STP37540S.

[23] C. Anghel. *Modified oxygen and hydrogen transport in Zr-based oxides*. Ph.D. thesis, KTH, 2006.

[24] J.-C. Brachet, I. Idarraga-Trujillo, M. L. Flem, et al. Early studies on Cr-Coated Zircaloy-4 as enhanced accident tolerant nuclear fuel claddings for light water reactors. *Journal of Nuclear Materials* **517**:268–285, 2019. https://doi.org/10.1016/j.jnucmat.2019.02.018.

[25] R. Pawel, J. Cathcart, R. McKee. The Kinetics of Oxidation of Zircaloy-4 in Steam at High Temperatures. *Journal of the Electrochemical Society* **126**(7):1105, 1979. https://doi.org/10.1149/1.2129227.

[26] R. Perkins. Oxygen diffusion in β-Zircaloy. *Journal of Nuclear Materials* **68**(2):148–160, 1977. https://doi.org/10.1016/0022-3115(77)90234-3.